The plastid division proteins, FtsZ1 and FtsZ2, differ in their biochemical properties and sub-plastidial localization

El-Sayed EL-KAFAFI*, Sunil MUKHERJEE*[1], Mahmoud EL-SHAMI*[2], Jean-Luc PUTAUX†, Maryse A. BLOCK‡, Isabelle PIGNOT-PAINTRAND†, Silva LERBS-MACHE* and Denis FALCONET*[3]

*Laboratoire de Génétique Moléculaire des Plantes, UMR 5575, CNRS-Université Joseph Fourier, BP 53, 38041 Grenoble, Cedex, France, †Centre de Recherches sur les Macromolécules Végétales (affiliated with the Université Joseph Fourier), UPR 5301-CNRS, BP 53, F-38041 Grenoble Cedex 9, France, and ‡Laboratoire de Physiologie Cellulaire Végétale, UMR 5168 CNRS–CEA–Université Joseph Fourier–INRA, CEA-Grenoble, DRDC-PCV, 17 rue des martyrs, 38054 Grenoble Cedex, France

Plastid division in higher plants is morphologically similar to bacterial cell division, with a process termed binary fission involving constriction of the envelope membranes. FtsZ proteins involved in bacterial division are also present in higher plants, in which the *ftsZ* genes belong to two distinct families: *ftsZ1* and *ftsZ2*. However, the roles of the corresponding proteins FtsZ1 and FtsZ2 in plastid division have not been determined. Here we show that the expression of plant FtsZ1 and FtsZ2 in bacteria has different effects on cell division, and that distinct protein domains are involved in the process. We have studied the assembly of purified FtsZ1 and FtsZ2 using a chemical cross-linking approach followed by PAGE and electron microscopy analyses of the resulting polymers. This has revealed that FtsZ1 is capable of forming long rod-shaped polymers and rings similar to the bacterial FtsZ structures, whereas FtsZ2 does not form any organized polymer. Moreover, using purified sub-plastidial fractions, we show that both proteins are present in the stroma, and that a subset of FtsZ2 is tightly bound to the purified envelope membranes. These results indicate that FtsZ2 has a localization pattern distinct from that of FtsZ1, which can be related to distinct properties of the proteins. From the results presented here, we propose a model for the sequential topological localization and functions of green plant FtsZ1 and FtsZ2 in chloroplast division.

Key words: chloroplast, chloroplast division, chloroplast envelope, FtsZ, FtsZ polymerization, stroma.

INTRODUCTION

The chloroplast division machinery in plants is an evolutionary hybrid, which has retained the activity of several prokaryotically derived proteins together with components that have evolved from proteins present in the eukaryotic ancestor [1,2]. Such a machinery is quite predictable from the endosymbiosis theory, which stipulates that the chloroplasts of plants originated just once from the cyanobacteria encapsulated by a biciliate protozoan [3]. Of the two membranes that immediately surround chloroplasts, the IEM (inner envelope membrane) was considered analogous to the plasma membrane of the symbiont, and the OEM (outer envelope membrane) was speculated to owe its dual origin to the host as well as to the symbiont [4].

The cyanobacterially derived proteins include FtsZ, the progenitor of tubulin, MinD and MinE, which mediate the placement of the division site on the stromal side of the IEM, ARTEMIS, which has a translocase function proposed to be involved in the integration of components into the IEM to enable chloroplast division, and ARC6, a J-domain plastid division protein, evolutionarily derived from the cyanobacterial cell division protein Ftn2 [2,5]. These proteins are localized inside the chloroplast, suggesting that the prokaryotically derived machinery is likely to be involved in the constriction of the IEM.

A second division machinery of eukaryotic origin has been postulated to be present at the surface of the organelle [6]. Recently, dynamins, which are not found in prokaryotes, have been shown to be involved in chloroplast division in the red alga *Cyanidioschyzon merolae* [7] and in *Arabidopsis thaliana* [8]. The localization experiments suggest that dynamin proteins form a ring at the chloroplast division site on the outer surface of the organelle.

Chloroplast division is an even more complex process, with the presence of an additional PD-ring (plastid dividing ring) associated with the region of constriction, as detected by TEM (transmission electron microscopy) [9]. The PD-ring is then resolved as an outer ring at the cytosolic face of the OEM and an inner ring on the stromal face of the IEM, and is thought to be ubiquitous in plant cells. In the red alga *Cyanidioschyzon merolae*, an additional middle ring is also present in the intermembrane space [10], but this ring has not been detected in plant chloroplasts. The biochemical, TEM and immunocytochemical analyses of the chloroplast division machinery in *Cyanidioschyzon merolae* and in the higher plant *Pelargonium zonale* Ait showed that the FtsZ and inner PD-rings are distinct [6]. The dynamin and the outer PD-rings have also been suggested to be distinct, on the basis of the molecular masses of the respective proteins implicated in the structure [7]. This raises the total number of rings involved in plastid division to five in *Cyanidioschyzon merolae*, compared with four in plants.

Besides the number of rings involved in plastid division, a major difference between the red and brown algae on the one hand and green organisms on the other is the presence of an additional FtsZ protein family in the latter organisms. In higher plants, phylogenetic analyses of FtsZ protein sequences indicate that FtsZ proteins are divided into two different groups called FtsZ1 and

Abbreviations used: IE37, inner envelope protein of 37 kDa; IEM, inner envelope membrane; IPTG, isopropyl β-D-thiogalactopyranoside; KARI, ketol–acid reducto-isomerase; LB, Luria–Bertani; OE24, outer envelope protein of 24 kDa; OEM, outer envelope membrane; PD-ring, plastid dividing ring; TEM, transmission electron microscopy.

[1] Present address: Plant Molecular Biology, International Centre for Genetic Engineering and Biotechnology, New Delhi 110067, India.
[2] Present address: Al Azha University, Faculty of Agriculture, Cairo, Egypt.
[3] To whom correspondence should be addressed (email denis.falconet@ujf-grenoble.fr).

FtsZ2 [11,12]. FtsZ1 is encoded by only one gene in *Arabidopsis thaliana* and by a gene family of at least four members in *Nicotiana tabacum* (an allotetraploid species). In both plants, a small multigene family encodes FtsZ2, with two members in *Arabidopsis thaliana*. It was demonstrated recently that the classification of FtsZ proteins into two distinct groups also extends to lower plants with green chloroplasts, while all the sequences analysed in other organisms form a single group [13,14]. The presence of two different FtsZ proteins in green plants (FtsZ1 and FtsZ2) raises the question of why the chloroplasts in these organisms need two different proteins in order to divide, when other organisms use only one protein.

To gain insight into the respective roles of FtsZ1 and FtsZ2 proteins in plastid division, we have analysed the effects of the expression of both proteins on bacterial division, and we have characterized the polymerization properties of the purified recombinant proteins *in vitro*. The results suggest that recombinant FtsZ1 and FtsZ2 proteins expressed in bacteria have different properties *in vivo* and *in vitro*. We have also determined the subplastidial localization of both proteins in plants. FtsZ2, in addition to being present together with FtsZ1 in the stroma, is also found tightly associated with the chloroplast envelope. Based on our observations, we propose a model outlining distinct roles of FtsZ1 and FtsZ2 in plastid division.

EXPERIMENTAL

Bacterial strains, plasmids, media and functional assays

Escherichia coli strain M15 was used as a host for expressing the plant *ftsZ1* and *ftsZ2* genes, cloned in the plasmid vector PQE31 (Qiagen). The recombinant plasmids PQE31-FtsZ1 and PQE31-FtsZ2 had been described previously and were used to overproduce the corresponding His_6–FtsZ fusion proteins, allowing the generation of the anti-FtsZ1 and anti-FtsZ2 specific antibodies employed in the present study [12]. The C-terminus of FtsZ2 was deleted by using the unique BamHI site present in the sequence. The resulting cDNA missing the last 82 codons was subcloned into PQE31. For functional assays, cells were grown in LB (Luria–Bertani) medium at 37 °C to early exponential phase. IPTG (isopropyl β-D-thiogalactopyranoside; 1 mM) was then added. Cells were grown for an additional 3 h, then samples were placed directly on glass slides and viewed on a Zeiss Axioplan 2 optical microscope, under a 60× oil immersion objective with phase contrast optics. Images were obtained with a video camera and Axiovision 3.1 software. For immunoblotting analyses, *E. coli* M15 proteins were separated by SDS/PAGE, blotted on to Immobilon-P membranes (Millipore) and reacted with the anti-histidine antibody (Pharmacia).

FtsZ protein purification

Nicotiana tabacum FtsZ1 and FtsZ2 proteins were expressed from a PQE31 vector (Qiagen) in *E. coli* strain M15 [12]. The bacteria were grown in LB medium at 37 °C to an absorbance (at 600 nm) of 0.6 before the addition of IPTG (0.5 mM final), and then grown for an additional 3 h at 37 °C. Bacteria were harvested by centrifugation, resuspended in lysis buffer (20 mM Tris/HCl, pH 7.5, 200 mM NaCl, 5 mM imidazole, 6 M urea, 1 μM leupeptin, 1 μM pepstatin A, 1 mM PMSF) and lysed by two passages through a French press. The lysate was cleared by centrifugation at 10000 ***g*** for 20 min and then chromatographed through a 0.5 ml column of nitrilotriacetic acid–agarose containing immobilized Ni^{2+} ions. The column was washed once with 20 column volumes (10 ml) of wash buffer (lysis buffer supplemented with 20 mM imidazole), then with a 50 ml linear gradient of urea (6 to 0.5 M) in wash buffer and finally with 10 ml of wash buffer without urea. Bound proteins were eluted with elution buffer [20 mM Tris/HCl, pH 7.5, 100 mM NaCl, 250 mM imidazole, 1 μM leupeptin, 1 μM pepstatin A, 1 mM PMSF, 1 mM dithiothreitol, 10 % (v/v) glycerol]. Fractions containing the recombinant proteins were pooled and dialysed against 20 mM Tris/HCl, pH 7.5, 100 mM NaCl, 10 mM benzamidine and 1 mM β-mercaptoethanol. The purity of the recombinant proteins was analysed further by SDS/PAGE and showed no major contamination with *E. coli* proteins.

FtsZ polymerization

Reaction mixtures (60 μl) containing FtsZ1 (200 $\mu g \cdot ml^{-1}$ or FtsZ2 (200 $\mu g \cdot ml^{-1}$) were incubated in the polymerization buffer (20 mM Tris/HCl, pH 7.5, 100 mM NaCl, 8 mM $MgCl_2$, 8 mM $CaCl_2$, 8 mM GTP) for 20 min at 27 °C and were allowed to continue without any treatment or with 0.1 % glutaraldehyde (ultrapure TEM grade; Sigma) for 2 min. The reactions were stopped by the addition of SDS (1 %, final). Samples of the polymerization reaction were resolved on an SDS/8%-polyacrylamide gel, blotted on to Immobilon-P membranes and probed with the anti-FtsZ1 or anti-FtsZ2 antibodies (1:100 dilution).

TEM

Droplets of 0.01 % (w/v) protein suspensions obtained from the polymerization reactions were deposited on to glow-discharged carbon-coated TEM grids. A drop of 2 % (w/v) uranyl acetate negative stain was added prior to complete drying. After 3 min, the liquid in excess was blotted and the remaining film was allowed to dry. The specimens were observed using a Philips CM200 microscope operated at 80 kV. Images were recorded on Kodak S0163 films at a magnification of 38000×.

Chloroplast protein fractionation, treatments and immunoblotting analyses

Intact chloroplasts were obtained from spinach (*Spinacia oleracea* L.) leaves and purified by isopycnic centrifugation using Percoll gradients [15]. The stroma, the thylakoids and the envelope fraction containing both outer and inner membranes were purified from lysed chloroplasts by centrifugation through a sucrose step gradient as described in [16]. Envelope subfractions enriched respectively in the outer or inner membrane were obtained as described [17]. Purified envelope membranes from thermolysin-treated chloroplasts were prepared as described in [18]. Briefly, Percoll-purified intact chloroplasts (final concentration 1 mg of chlorophyll $\cdot ml^{-1}$) were incubated in medium containing 0.3 M sucrose, 10 mM tricine/NaOH, pH 7.8, and 1 mM $CaCl_2$ for 1 h at 4 °C with various concentrations of thermolysin from *Bacillus thermoproteolyticus* (Calbiochem). The digestion was terminated by the addition of 10 mM EGTA. The control (no thermolysin) and treated (100 μg or 600 μg of thermolysin $\cdot ml^{-1}$) intact chloroplasts were recovered on a second Percoll gradient to prepare the corresponding total envelope fractions.

Chloroplast envelope proteins were extracted using alkaline or salt treatments. The total envelope fraction (30 μg of protein) was incubated for 30 min at 0 °C in 10 mM Mops, pH 7.8, or 10 mM Mops, pH 7.8/1 M NaCl, or 0.1 M Na_2CO_3, pH 11, or 0.1 M NaOH. The mixtures were then centrifuged at 100000 ***g*** for 30 min and the pellets and the supernatants were separated. The pellets and the trichloroacetic acid-precipitated proteins from the supernatant were resuspended in 1 × Laemmli sample buffer.

For immunoblotting analyses, the proteins were separated by SDS/PAGE, blotted on to Immobilon-P membranes and allowed to react with the antibodies as described previously [12].

Immunogold electron microscopy

For immunogold electron microscopy, purified spinach chloroplasts were fixed in 2.5 % (v/v) glutaraldehyde in 0.1 M PBS for 1 h at 4 °C. The chloroplasts were washed for 3 × 10 min in PBS, treated with 2 % OsO_4 for 1 h, dehydrated in an ethanol gradient and embedded in Epon. Ultrathin sections were cut with a diamond knife on a Reichert ultramicrotome and collected on nickel grids. The sections were etched with 10 % H_2O_2, blocked with 5 % (w/v) BSA and incubated with the anti-FtsZ2 antibody (dilution 1:4 in PBS/1 % BSA) overnight at 4 °C. Secondary reactions were performed for 1 h at 20 °C with goat anti-(rabbit IgG) conjugated with 5 nm colloidal gold (British Biocell) at a dilution of 1:20 in PBS/1 % BSA. Sections were observed by electron microscopy.

RESULTS

FtsZ1 and FtsZ2 proteins have different effects on *E. coli* cell division

To determine if plant FtsZ1 and FtsZ2 influence *E. coli* cell division, we examined the effects of both FtsZ proteins by overproducing them in *E. coli* M15 by employing the expression vector PQE31. In this plasmid the protein is fused to a small histidine tag, and such small tags have been shown not to interfere with the biological activities of bacterial FtsZ [19,20]. In the absence of IPTG, the proteins were not expressed, as shown by Western blot with anti-histidine antibodies (Figure 1A). The growth rate (Figure 1B) and cell morphology of bacteria harbouring PQE-FtsZ1 (Figure 1C) and PQE-FtsZ2 (results not shown) appeared to be similar. In the presence of IPTG, both proteins were overexpressed and different bacterial behaviours were observed. When FtsZ2 was overexpressed, a sharp decrease in growth rate starting from the beginning of the induction period (Figure 1B) was concomitant with a change in cell morphology, with the presence of long filaments (Figure 1E). In contrast, FtsZ1 overexpression did not affect the growth rate during the first 2 h after induction. A decrease in growth rate was only observed after 3 h of protein induction, with the formation of multinucleate cells (Figure 1D), similar to cells observed when bacterial FtsZ is overexpressed in *E. coli* [21]. In order to test if the drastic effect with FtsZ2 is related to the presence in the C-terminus of FtsZ2, but the absence from FtsZ1, of elements known to be important for interaction with other proteins (see Discussion), we deleted part of the C-terminal region of FtsZ2. The truncated protein (FtsZ2D) was detected with the antibody when protein expression is induced with IPTG. The growth rate of the bacteria producing the truncated proteins was higher than the growth rate observed for bacteria expressing the full-length protein, and the number of viable cells of *E. coli* producing the truncated protein was increased over 10-fold relative to the cells producing full-length FtsZ2 (results not shown). As observed in Figure 1(F), the morphology of the bacteria was also different, with no long filaments as were observed with full-length FtsZ2, and the absence of multinucleate cells as was observed with FtsZ1.

FtsZ1 and FtsZ2 proteins have different polymerization properties *in vitro*

To study the structural and functional properties of chloroplast FtsZ1 and FtsZ2 proteins, polymerization reactions were performed with the recombinant proteins purified as described in the Experimental section. The polymerization products were analysed using a chemical cross-linking approach [22]. After 20 min of polymerization, 2 min of cross-linking with 0.1 % (v/v) glutaraldehyde was performed to stabilize and cross-link the polymers. The reactions were then stopped by the addition of 1 % (v/v) SDS and the reaction products were separated by SDS/PAGE, transferred on to a membrane and detected with the specific antibodies against FtsZ1 and FtsZ2. After 20 min of polymerization and cross-linking, a drastic decrease in the FtsZ1 monomer concentration was observed (Figure 2A, lane 3). Such a decrease was not observed in the absence of glutaraldehyde (Figure 2A, lane 2). A kinetic reaction analysis was performed in order to determine whether the disappearance of the monomers was progressive and if the absence of polymerization products was the result of a rapid polymerization process, giving rise to high-molecular-mass polymers that could not enter the gel (Figure 2B). After 4 min of polymerization, FtsZ1 structures of intermediate molecular mass (90–350 kDa) were detected in the resolving part of the gel; subsequently, these structures were not detected as the monomer concentration decreased rapidly. After 30 min of

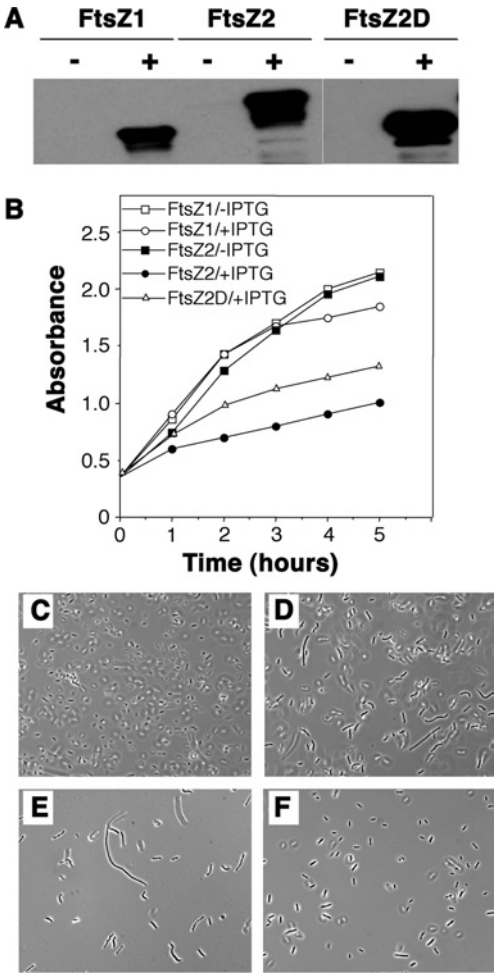

Figure 1 Effects of His_6-tagged FtsZ1, FtsZ2 and C-terminally truncated FtsZ2 (FtsZ2D) on *E. coli* M15 cell growth and division

(**A**) Cells were grown to early exponential phase before the addition, or not, of IPTG (1 mM final), and overexpression of the proteins was determined using an anti-histidine antibody after 3 h of growth in the absence (−) or presence (+) of IPTG. (**B**) Aliquots were removed for absorbance reading at 600 nm. Cells were photographed after 3 h of growth in the absence (**C**) or presence of 1 mM IPTG inducing the expression of FtsZ1 (**D**), FtsZ2 (**E**) and truncated FtsZ2 (**F**).

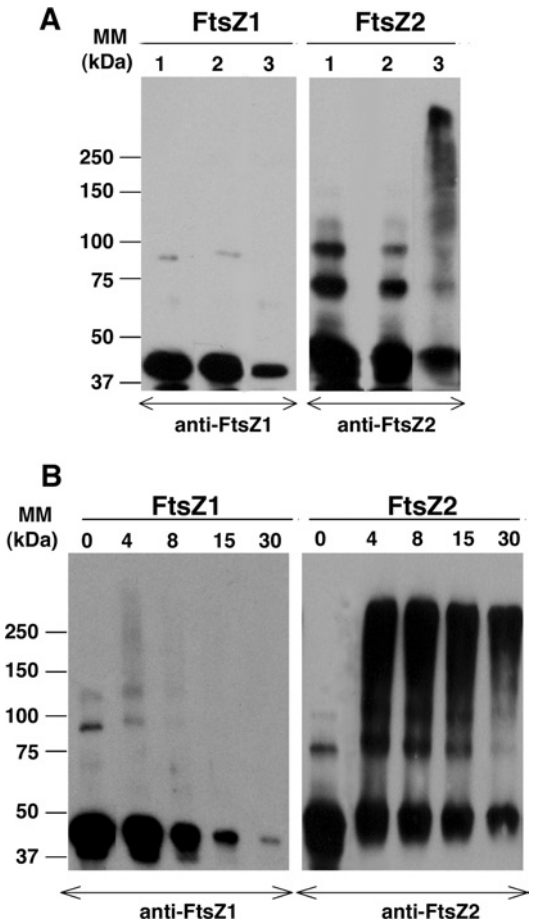

Figure 2 Cross-linking of FtsZ1 and FtsZ2 polymerization products

(**A**) Reaction mixtures (60 μl) containing FtsZ1 or FtsZ2 were incubated in polymerization buffer for 20 min without treatment (lane 2) or after chemical cross-linking (lane 3) with the addition of glutaraldehyde. FtsZ protein (1 μg; lane 1) together with samples of the polymerization reaction (5 μl) were resolved on an SDS/8 %-glutaraldehyde gel and subsequently blotted on to Immobilon-P membranes and probed with the indicated antibodies. (**B**) Kinetics of FtsZ1 and FtsZ2 polymerization. Polymerization reactions were performed with the addition of glutaraldehyde. Aliquots of the reaction mixture were withdrawn at different times (min; shown above each lane) and polymer formation was monitored as described above with anti-FtsZ1 or anti-FtsZ2 antibody. MM, molecular mass.

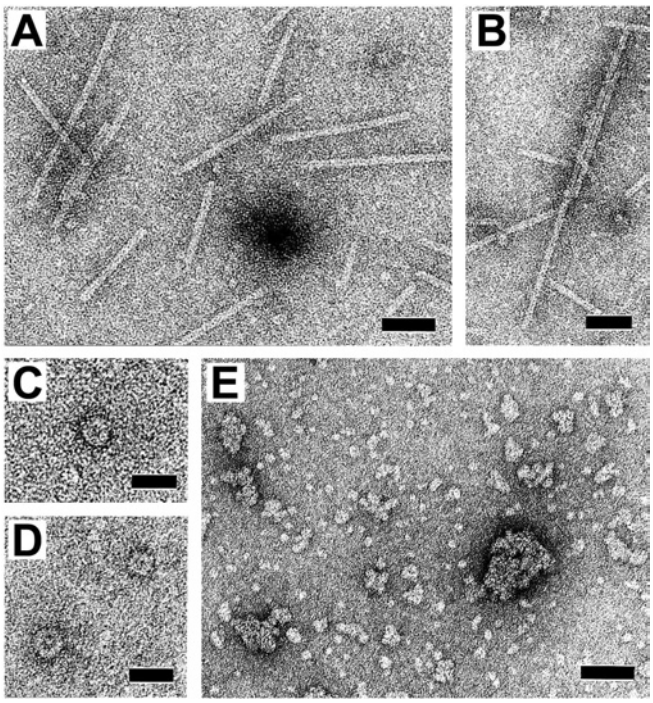

Figure 3 TEM observation of FtsZ1 and FtsZ2 assembly

Typical TEM images are shown of the products of plant FtsZ1 (**A**–**D**) and FtsZ2 (**E**) polymerization reactions analysed in Figure 2. Structures were visualized after negative staining. The scale bars correspond to 50 nm in (**A**), (**B**) and (**E**), and to 20 nm in (**C**) and (**D**).

polymerization, FtsZ1 monomers were almost absent from the reaction mixture. Altogether, these observations were consistent with the formation of high-molecular-mass polymers from FtsZ1. Under the same reaction conditions, FtsZ2 behaved differently. Although concomitant with the appearance of some structures of intermediate molecular mass, the decrease in the FtsZ2 monomer concentration in the presence of glutaraldehyde was far less than that observed for FtsZ1, suggesting that there was no formation of high-molecular-mass polymers from FtsZ2 (Figure 2A, lane 3 and Figure 2B).

TEM of negatively stained samples was used to characterize the FtsZ structures generated by the different polymerization reactions. As seen in Figure 3(A), images of FtsZ1 samples taken after 20 min of polymerization revealed rod-like single-stranded protofilaments with a cross-sectional width of 5–7 nm and an average length of 120–150 nm. The polydispersity in length of the rods was high; filaments as short as 30 nm or as long as 550 nm could be observed. A 450 nm-long filament is shown in Figure 3(B). In addition to straight protofilaments, ring-shaped polymers were also formed with an average diameter of 13 nm (Figures 3C and 3D). In contrast, TEM images of FtsZ2 samples did not reveal any protofilaments (Figure 3E). More or less aggregated globular objects were observed that did not have any recognizable shape or structure. These aggregates were not observable in the absence of glutaraldehyde and probably represent cross-linked structures.

The polymers formed with the plant chloroplast protein FtsZ1 are similar to those formed with bacterial FtsZ. When tested under the same polymerization conditions, bacterial FtsZ assembles into single, straight protofilaments, 5 nm in diameter [19,23], and mini-rings, 23 nm in diameter, which were identified as protofilaments in the curved conformation [24]. In conclusion, FtsZ2 was unable to polymerize under conditions that promoted the rapid assembly of plant FtsZ1.

Polymerization of bacterial FtsZ was found to be dependent on GTP [25,26]. To investigate whether polymerization of plant FtsZ1 is also nucleotide-dependent, polymerization assays were performed in the presence or absence of GTP. The polymerization products were analysed using the chemical cross-linking approach. As observed in Figure 4, after 30 min of polymerization in the presence of GTP, FtsZ1 monomers were not detected with the anti-FtsZ1 antibody, indicating that FtsZ1 polymerization had occurred. In contrast, in the absence of GTP in the reaction mixture, no polymerization occurred, as shown by the detection of FtsZ1monomers, thus indicating that FtsZ1 polymerization is GTP-dependent. Under the same conditions, in the presence or absence of GTP in the FtsZ2 polymerization reaction mixture, the same cross-linked structures as observed in Figure 2 were also detected with the anti-FtsZ2 antibody in both reactions (Figure 4). Interestingly, when the polymerization reactions were performed in the presence of both proteins, FtsZ1 polymerization occurred even in the absence of GTP, since no FtsZ1 monomer was detected. The presence of FtsZ1 had no effect on FtsZ2 polymerization.

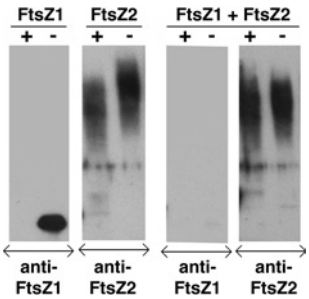

Figure 4 FtsZ2 promotes the assembly of FtsZ1 in the absence of GTP

Reaction mixtures containing FtsZ1, FtsZ2 or FtsZ1 plus FtsZ2 were incubated in polymerization buffer in the presence (+) or absence (−) of GTP for 30 min. Products were analysed as described in the legend to Figure 2 with anti-FtsZ1 or anti-FtsZ2 antibodies.

Thus plant FtsZ2, which itself is unable to polymerize, induces polymerization of FtsZ1 in the absence of GTP.

FtsZ1 and FtsZ2 are localized within the stroma, but FtsZ2 is also found associated with the chloroplast envelopes

In order to test whether the different polymerization properties of FtsZ1 and FtsZ2 are related to differences in their sublocalization within the organelle, we have re-evaluated the localization of FtsZ1 and FtsZ2 in plant chloroplasts. All members of the FtsZ1 family are predicted by the program TargetP to contain cleavable chloroplast transit peptides at their N-terminal ends that should target them to the stromal compartment [27]. Using an *in vitro* import assay, it was shown that FtsZ1 proteins from *Arabidopsis* [1] and pea [22] are imported into isolated chloroplasts and processed to the mature form. In contrast, the targeting scores for FtsZ2, ranging from 0.131 for *Nicotiana tabacum* FtsZ2 to 0.732 for *Lilium longiflorum* FtsZ2, are more equivocal, revealing a potentially important distinction between plant FtsZ1 and FtsZ2 proteins [27].

In the present study we have investigated the localization of both FtsZ proteins by Western blotting of protein extracts derived from spinach chloroplasts. The stroma, thylakoid and envelope fractions were purified by classical methods and envelope subfractions were shown to be highly enriched in IEM and OEM respectively, as indicated by immunological studies (Figure 5A) using polypeptides markers for each membrane, i.e. IE37 (inner envelope protein of 37 kDa) for IEM and OE24 (outer envelope protein of 24 kDa) for OEM [17,28]. Signals were observed with the anti-FtsZ1 and anti-FtsZ2 antibodies, which reacted with the protein extracts derived from chloroplasts and from the stromal fraction (Figure 5A, lanes 1 and 3). No signal was observed with proteins in the thylakoid fraction (Figure 5A, lane 2). Interestingly, an immunoreactive signal with the anti-FtsZ2 antibody, but not with the anti-FtsZ1 antibody, was also observed with both the IEM and OEM protein extracts (Figure 5A, lanes 4 and 5). In order to test if this signal was due to contamination with stromal proteins, a control was performed with KARI (ketol–acid reductoisomerase; also known as acetohydroxy acid isomeroreductase), a stromal protein involved in the biosynthetic pathway of amino acids [29]. As expected, a strong signal was observed in the stromal fraction at a size corresponding to mature KARI. With both IEM and OEM, two bands were detected, with the lower band corresponding to the mature protein and the upper band to the precursor protein. The signal for the precursor protein was present mainly in the OEM. The faint signals observed with the mature protein in both the IEM and OEM are a good indication of the low level of contamination of the envelope preparations

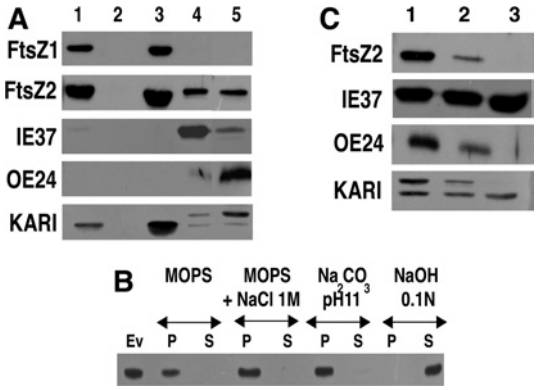

Figure 5 Chloroplast sublocalization of plant FtsZ1 and FtsZ2 proteins

(**A**) Western blot analysis of protein fractions (30 μg of each) from chloroplasts (lane 1), thylakoids (lane 2), stroma (lane 3), IEM (lane 4) and OEM (lane 5) with antibodies against plant FtsZ1 and FtsZ2 proteins, IE37, OE24 and KARI (a stromal protein). (**B**) Purified plastid envelopes (30 μg of protein) were incubated for 30 min in the indicated media and the proteins were separated into insoluble (P) and soluble (S) fractions. These fractions, together with purified envelope proteins (Ev), were fractionated by SDS/PAGE, blotted and reacted with the anti-FtsZ2 antibody. (**C**) Purified envelopes from control chloroplasts (lane 1) and from chloroplasts treated with 100 $\mu g \cdot ml^{-1}$ (lane 2) or 600 $\mu g \cdot ml^{-1}$ (lane 3) thermolysin were probed with antibodies against FtsZ2, IE37, OE24 and KARI.

with stromal proteins. The observation that the FtsZ2 signal in both membrane subfractions was above the stromal contamination background level indicates that a subset of FtsZ2 protein was also associated with both plastid envelope membranes. To characterize further the association of FtsZ2 with the envelope, the fraction containing both membranes was isolated and washed with 1 M NaCl, 0.1 M Na_2CO_3, pH 11, or 0.1 M NaOH. The FtsZ2 proteins were released from the membranes only by treatment with NaOH, but not by any of the other reagents (Figure 5B). Therefore we concluded that the envelope-localized FtsZ2 protein was bound firmly to the envelope membranes.

In order to define further the topological association of FtsZ2 with the plastid envelope, thermolysin digestion of isolated intact chloroplasts was performed. After treatment with two different concentrations of thermolysin, chloroplasts were re-isolated on Percoll gradients. The purified envelope membranes were separated and the constituent polypeptides were tested by Western blotting. As shown in Figure 5(C), both FtsZ2 and OE24 were protease-sensitive, and neither of these two proteins was apparent after treatment with the high thermolysin concentration. In contrast, IE37, the IEM protein, was not modified by protease treatment, confirming the intactness of the chloroplasts during the incubation. As observed in Figure 5(C), mature and precursor KARI proteins behaved differently on thermolysin treatment. The mature protein was not affected by the protease, while the precursor was fully degraded after treatment with the higher thermolysin concentration. This result is in good agreement with the conclusion that stromal proteins are not affected by the protease, whereas the precursor protein, which remains associated with the envelope membranes and extends outside the chloroplast, is sensitive [30]. The susceptibility of the envelope-bound FtsZ2 to protease treatment, in contrast with the absence of degradation of the stromal protein contaminant, confirms the localization of this FtsZ2 protein subset within the plastidial envelope.

To confirm visually the dual localization of FtsZ2 within the chloroplast, immunoelectron microscopy was performed. Intact purified chloroplasts were visualized by electron microscopy in order to verify chloroplast integrity (Figure 6A). The subplastidial localization of FtsZ2 was demonstrated using immunogold techniques. Clusters of gold particles were observed within

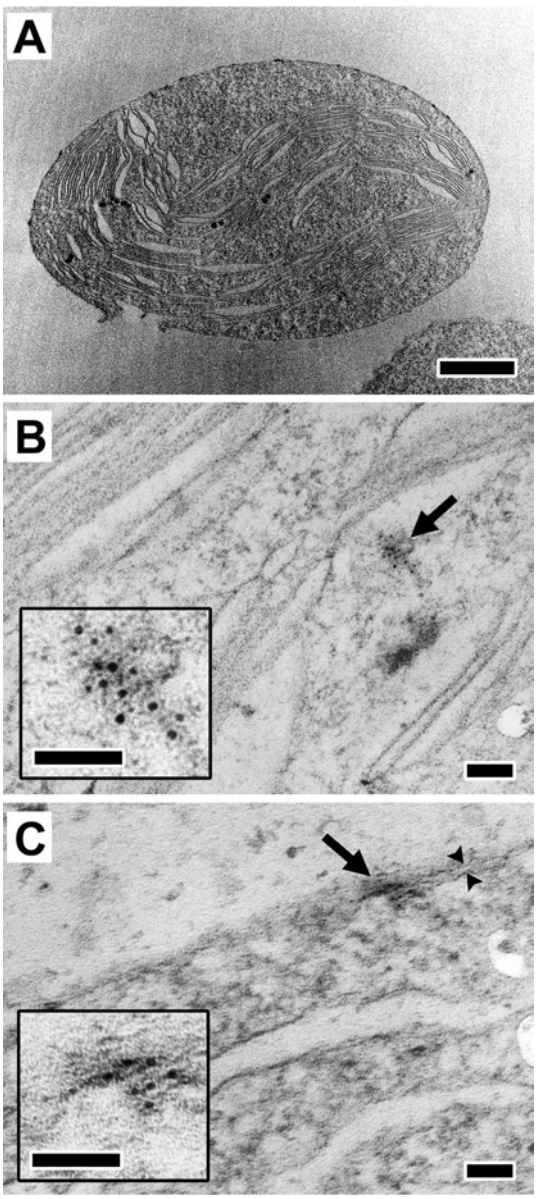

Figure 6 Sub-plastidial localization of FtsZ2 using immunogold techniques

Intact spinach chloroplasts were immobilized, fixed and observed under electron microscopy (**A**) or incubated successively with anti-FtsZ2 antibody and goat anti-(rabbit IgG) conjugated to colloidal gold. Panels (**B**) and (**C**) show FtsZ2 labelling within the chloroplast and in contact with the chloroplast envelope respectively. Higher-magnification images of the gold clusters indicated with the arrows are shown in the bottom left corners in (**B**) and (**C**). The IEM and OEM are indicated by arrowheads in (**C**). The scale bars correspond to 1 μm in (**A**) and 50 nm in (**B**) and (**C**).

the chloroplast (Figure 6B), and probably represent the stromal fraction. In addition, clusters were also observed, albeit less frequently, at the chloroplast periphery, in close association with the chloroplast envelope (Figure 6C), confirming the dual localization of FtsZ2.

Taken together, our results demonstrate that (1) FtsZ1 and a major subset of FtsZ2 were localized within the stroma, and that (2) another, small subset of FtsZ2 was strongly associated with both the IEM and the OEM of the plastid envelope. This association was affected by proteolytic treatment of the chloroplast surface.

DISCUSSION

The aim of our present work was to use both *in vivo* and *in vitro* methods to unravel the similarities and/or differences in functional behaviour and biochemical properties of the two plant FtsZ proteins. In addition, we have re-evaluated the sub-plastidial localization of FtsZ1 and FtsZ2. We show that expression of FtsZ1 and FtsZ2 *in vivo* affects *E. coli* division in different ways. The division of bacteria expressing His_6-tagged plant FtsZ1 was only impaired when the protein was expressed to a high level, with the formation of longer filaments, mimicking the effects of expression of other bacterial *ftsZ* genes in *E. coli* [31]. In contrast, FtsZ2 expression drastically inhibited cell division, suggesting differences in the interactions of the plant FtsZ1 and FtsZ2 proteins with the bacterial division apparatus. Since even low expression of FtsZ2 had marked effects on bacterial division, this suggests a competitive effect between the bacterial FtsZ and plant FtsZ2 proteins. All FtsZ2 sequences (but not those of FtsZ1) contain, in common with bacterial FtsZ, a short conserved peptide in the C-terminal region that is known to bind two other proteins, ZipA and FtsA, required for *E. coli* cell division [32]. ZipA is an integral membrane protein that serves as a membrane anchor for the FtsZ ring and may also stabilize and cross-link FtsZ polymers [33]. FtsA, which lacks a clear membrane-spanning sequence, is a peripheral membrane protein related to the actin/Hsp70 superfamily of ATPases [34]. Once bound to the FtsZ, FtsA may form a bridge between the ring and membrane-anchored proteins of the divisome, recruiting other cell division proteins to the division site. To address the activity of the FtsZ2 C-terminal sequence, expression of truncated FtsZ2 was performed. Our results suggested that the deleted sequence interferes with the bacterial division apparatus and that some of the negative effects of FtsZ2 on bacterial division are related to the presence of this conserved C-terminal domain, which blocks further bacterial division. Neither ZipA nor FtsA has been identified in plant or cyanobacteria on the basis of sequence similarity [2,5]. The observed effect of the FtsZ2 C-terminus on bacterial division suggests the presence of as yet unidentified proteins that interact specifically with FtsZ2. Taken together, our results suggest that plant FtsZ1 and FtsZ2 affect bacterial division via different mechanisms involving distinct protein domains.

Like tubulin, bacterial FtsZ has the capacity to polymerize *in vitro* into polymers with structural features that are similar to those of microtubules [19,23,26]. Both proteins bind and hydrolyse GTP to form polymers with similar lattice structures [24]. When tested under a variety of *in vitro* conditions, FtsZ assembles into single, straight protofilaments, sheets of straight protofilaments, mini-rings and tubular polymers [24–26,35,36], thus providing insight into potential structures and functions *in vivo* [37].

We have shown that plant FtsZ1, but not FtsZ2, is able to polymerize, and that the polymerization is GTP-dependent. Only images of FtsZ1 samples revealed structures similar to those observed with bacterial FtsZ. The aggregates detected by gel analysis of FtsZ2 were likely to be non-organized structures resulting from cross-linking, as shown by their absence when no glutaraldehyde was added. It is not yet known whether polymerization of FtsZ2 *in vitro* requires conditions different from those required by FtsZ1, or whether the *in vitro* conditions simulate the *in vivo* conditions. Nevertheless, our results indicate that, using conditions permissible for bacterial FtsZ polymerization, plant FtsZ1 polymerizes efficiently, while FtsZ2 fails to do so. The inability of FtsZ2 to polymerize might reflect a different role for this protein in chloroplast division. Indeed, we show here that, in the absence of GTP, FtsZ2 promotes the assembly of FtsZ1.

In *Bacillus subtilis*, a Z-ring-associated protein called ZapA was capable of binding to FtsZ and was shown to promote FtsZ polymerization in the absence of GTP [38]. ZapA is widely conserved in bacteria, but no orthologue is present in plant genomes. Our results suggest that FtsZ2 might fulfil this function in the formation of the FtsZ1 ring.

Localization of higher-plant FtsZ1 and FtsZ2 proteins in the stromal compartment of the chloroplast has been shown in two independent studies. In the first, a biochemical approach was used to show that the two *Arabidopsis* FtsZ2 proteins, like FtsZ1, are imported into isolated chloroplasts, processed to mature forms and protected from proteolytic degradation following import [39]. The sub-organellar localization of both *in vitro*-imported and endogenous FtsZ1 and FtsZ2 proteins was analysed by protease protection assays. The authors provided strong evidence that both proteins were localized in the stromal compartment of the chloroplast. In the second study, it was shown by immuno-electron microscopy that both FtsZ1 and FtsZ2 were present in the inner stromal region in the chloroplasts of cotyledon cells from early embryos of *Pelargonium zonale* Ait [40]. Using purified chloroplast subfractions, our results demonstrate that FtsZ1 is localized only in the stroma; on the other hand FtsZ2, although present in large amounts in the stroma fraction, was also found associated with the envelope membranes. The signal observed for FtsZ2 in the envelope fractions was above the level of background contamination, as tested using KARI, a stromal protein. Moreover, FtsZ2 was tightly associated with the envelope, since only washing of the membranes with NaOH was able to release FtsZ2 into the soluble fraction. FtsZ2 protein was found associated equally with both membranes, i.e. the IEM and the OEM. Cross-contamination between the IEM and OEM fractions cannot explain this equal partitioning, in view of the enrichment of marker protein for each membrane. In order to analyse the topological association of FtsZ2 with the OEM, controlled thermolysin treatments of intact chloroplasts were performed and the susceptibility of FtsZ2 to digestion was compared with that of control proteins. Surprisingly, FtsZ2 behaved similarly to OE24, a control protein accessible to the cytosolic side of the OEM. The two proteins disappeared completely from the envelopes, whereas IE37 (which is associated with the IEM) and the KARI mature protein were not affected by protease treatment. The membrane-bound FtsZ2 behaved in a similar fashion as the KARI precursor protein. Such chloroplast precursor proteins have been found to be associated with both the IEM and the OEM, and to be susceptible to thermolysin treatment. The model proposed to take these data into account is that protein translocation proceeds at contact sites where the OEM and IEM are closely apposed [30]. The molecular mass of the membrane-bound FtsZ2 corresponded to that of the mature protein, thus ruling out the possibility that the detected FtsZ2 is an import intermediate. Similarly to the above model, a hypothetical explanation for the envelope localization of FtsZ2, and its disappearance after protease treatment, is that FtsZ2 is part of a protein continuum extending from the IEM to the cytosolic side of the OEM at a site where the two membranes are closely apposed. This continuum would generate a physical link from the outside to the inside of the chloroplast, thus allowing formation of the division site at this constriction point.

In view of the results presented here and previously published models concerning plastid division [6,7,27,39], we propose the following sequence of events for the localization and functions of the green plant FtsZ1 and FtsZ2 proteins (Figure 7). At the beginning of division, a subset of FtsZ2 is localized at the future division site. This membrane-bound FtsZ2, in association or not with other proteins, forms a protein continuum spanning both membranes

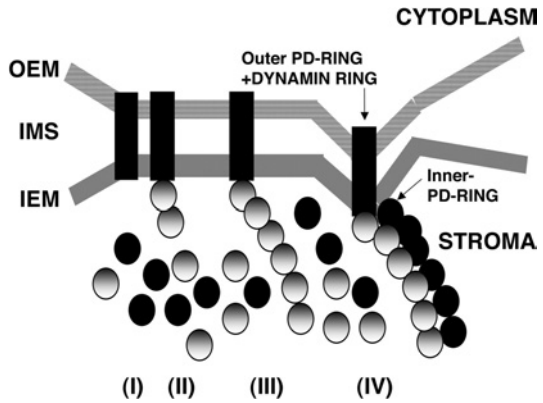

Figure 7 Proposed sequence of events during chloroplast division

Stage I: localization of FtsZ2 at a contact site between the OEM and IEM. FtsZ2, in association or not with other proteins, forms a protein bridge spanning the two membranes and connecting the outside surface of the chloroplast to the stroma (black rectangles). Stage II: interaction of FtsZ1 (grey circles) with the membrane-bound FtsZ2 protein complex. Stage III: formation of the FtsZ1 ring. Stage IV: FtsZ2 (black circles) interacts with the FtsZ1 ring, allowing the recruitment of new proteins and the formation of the inner PD-ring. Concomitantly, or soon afterwards, the outer PD-ring and the dynamin ring are formed on the cytoplasmic side of the chloroplast. IMS, inner membrane space.

(shown as a black box in Figure 7). The presence of such a protein link, extending from the outside to the inside of the chloroplast, allows the co-localization of the internal and the external division apparatus. In the red alga *Cyanidioschyzon merolae*, an additional middle ring is present in the intermembrane space [10], but this has not been detected in plant chloroplasts. Whether FtsZ2 fulfils this function in green plants is not yet known. Concomitantly with or shortly after this initiation step, FtsZ1 is recruited to the division site and forms an annular structure similar to the bacterial FtsZ ring. Given its presence in large amounts in the stroma, FtsZ2 may have additional functions in FtsZ1 ring formation. FtsA, present in various bacterial species, but not in cyanobacteria or plants, has been shown in *E. coli* to co-localize with FtsZ in a circumferential ring at the division site by immunofluorescence studies [41] and by examination of an FtsA fusion with green fluorescent protein [42]. One specific role for FtsA is the recruitment of other cell division proteins to the division site. Therefore FtsZ2, after interacting with the FtsZ1 ring, may help to promote Z-ring formation, and then recruit additional proteins and participate in the placement of the inner PD-ring, located between the Z-ring and the IEM [6]. Finally, the outer PD-ring and the dynamin ring are formed, leading to plastid division.

In conclusion, the model we propose here considers: (i) a role for FtsZ2 in the co-localization in the same spatial plane of the IEM and OEM constriction sites prior to plastid division; (ii) a further role for FtsZ2 in the subsequent formation of the FtsZ ring in the stroma; and (iii) the involvement of FtsZ2 in recruiting additional proteins at the division site.

The various functions associated with FtsZ2 are in agreement with previously published results concerning plant FtsZ1 and FtsZ2 proteins. The *ftsZ2* gene families are more complex than *ftsZ1* families, with the presence of additional members and the presence of two discrete FtsZ2 polypeptides, as detected by Western blot [12,43]. FtsZ2 mRNAs and proteins have been shown to accumulate earlier than FtsZ1 mRNAs and proteins during the cell cycle in BY2 cells [12]. This earlier expression could be related to the involvement of FtsZ2 in the selection of the division sites before FtsZ1 polymerization occurs.

Since the discovery that plastids use FtsZ to divide, the question of why the green plant *ftsZ* genes had evolved to form two different families encoding two different proteins has not yet been answered. We show here that green plant FtsZ1 and FtsZ2 have different biochemical properties and plastidial sub-localizations, and propose specific functions for the two proteins in plastid division. Further studies are needed to determine the contribution of each FtsZ2 protein (encoded by two different genes in *Arabidopsis*) in relation to their sub-localization. Characterization of the respective mutants should help to clarify this point.

We thank Renaud Dumas (PCV, Grenoble) for the gift of the anti-KARI antibody. We thank Hélène Pesey for technical assistance and Paul Mandaron for help with electron microscopy. We thank Dr Roberto Geremia for critical reading of the manuscript. We also thank members of the LAPM laboratory (CERMO) for allowing us to use the Zeiss Axioplan 2 microscope. This work was supported by a grant (ACI DRAB 03/41, no. 03 5 90) from the Centre National de la Recherche Scientifique (CNRS) and the Ministère de l'Education Nationale (MEN). M.E.-K. and M.E.-S. are supported by the Ministère de l'Education Egyptien. S.M. was supported as an invited professor by Université Joseph Fourier.

REFERENCES

1 Osteryoung, K. W. and Vierling, E. (1995) Conserved cell and organelle division. Nature (London) **376**, 473–474
2 Miyagishima, S., Nishida, K. and Kuroiwa, T. (2003) An evolutionary puzzle: chloroplast and mitochondrial division rings. Trends Plant Sci. **8**, 432–438
3 Gray, M. W. (1993) Origin and evolution of organelle genomes. Curr. Opin. Genet. Dev. **3**, 884–890
4 Cavalier-Smith, T. (2000) Membrane heredity and early chloroplast evolution. Trends Plant Sci. **5**, 174–182
5 Osteryoung, K. W. and Nunnari, J. (2003) The division of endosymbiotic organelles. Science **302**, 1698–1704
6 Miyagishima, S., Takahara, M., Mori, T., Kuroiwa, H., Higashiyama, T. and Kuroiwa, T. (2001) Plastid division is driven by a complex mechanism that involves differential transition of the bacterial and eukaryotic division rings. Plant Cell **13**, 2257–2268
7 Miyagishima, S., Nishida, K., Mori, T., Matsuzaki, M., Higashiyama, T., Kuroiwa, H. and Kuroiwa, T. (2003) A plant-specific dynamin-related protein forms a ring at the chloroplast division site. Plant Cell **15**, 655–665
8 Gao, H., Kadirjan-Kalbach, D., Froehlich, J. E. and Osteryoung, K. W. (2003) ARC5, a cytosolic dynamin-like protein from plants, is part of the chloroplast division machinery. Proc. Natl. Acad. Sci. U.S.A. **100**, 4328–4333
9 Kuroiwa, T., Kuroiwa, H., Sakai, A., Takahashi, H., Toda, K. and Itoh, R. (1998) The division apparatus of plastids and mitochondria. Int. Rev. Cytol. **181**, 1–41
10 Miyagishima, S., Itoh, R., Toda, K., Takahashi, H., Kuroiwa, H. and Kuroiwa, T. (1998) Identification of a triple ring structure involved in plastid division in the primitive red alga *Cyanidioschyzon merolae*. J. Electron Microsc. **47**, 269–272
11 Osteryoung, K. W., Stokes, K. D., Rutherford, S. M., Percival, A. L. and Lee, W. Y. (1998) Chloroplast division in higher plants requires members of two functionally divergent gene families with homology to bacterial *ftsZ*. Plant Cell **10**, 1991–2004
12 El-Shami, M., El-Kafafi, S., Falconet, D. and Lerbs-Mache, S. (2002) Cell cycle-dependent modulation of FtsZ expression in synchronized tobacco BY2 cells. Mol. Genet. Genomics **267**, 254–261
13 Gilson, P. R. and Beech, P. L. (2001) Cell division protein FtsZ: running rings around bacteria, chloroplasts and mitochondria. Res. Microbiol. **152**, 3–10
14 Stokes, K. D. and Osteryoung, K. W. (2003) Early divergence of the FtsZ1 and FtsZ2 plastid division gene families in photosynthetic eukaryotes. Gene **320**, 97–108
15 Douce, R. and Joyard, J. (1982) Purification of the chloroplast envelope. In Methods in Chloroplast Molecular Biology (Edelman, M., Hallick, R. and Chua, N.-H., eds.), pp. 239–256, Elsevier Biochemical Press, Amsterdam
16 Douce, R., Holtz, R. B. and Benson, A. A. (1973) Isolation and properties of the envelope of spinach chloroplasts. J. Biol. Chem. **248**, 7215–7222
17 Block, M. A., Dorne, A. J., Joyard, J. and Douce, R. (1983) Preparation and characterization of membrane fractions enriched in outer and inner envelope membranes from spinach chloroplasts. I – Electrophoretic and immunochemical analyses. J. Biol. Chem. **258**, 13273–13280
18 Joyard, J., Block, M. A., Pineau, B., Albrieux, C. and Douce, R. (1990) Envelope membranes from mature spinach chloroplasts contain a NADPH:protochlorophyllide reductase on the cytosolic side of the outer membrane. J. Biol. Chem. **265**, 21820–21827
19 Lu, C. and Erickson, H. P. (1998) Purification and assembly of FtsZ. Methods Enzymol. **298**, 305–313
20 Lu, C., Stricker, J. and Erickson, H. P. (1998) FtsZ from *Escherichia coli*, *Azotobacter vinelandii*, and *Thermotoga maritima* – quantitation, GTP hydrolysis, and assembly. Cell Motil. Cytoskeleton **40**, 71–86
21 Ward, Jr, J. E. and Lutkenhaus, J. (1985) Overproduction of FtsZ induces minicell formation in *E. coli*. Cell **42**, 941–949
22 Gaikwad, A., Babbarwal, V., Pant, V. and Mukherjee, S. K. (2000) Pea chloroplast FtsZ can form multimers and correct the thermosensitive defect of an *Escherichia coli* ftsZ mutant. Mol. Gen. Genet. **263**, 213–221
23 Mukherjee, A. and Lutkenhaus, J. (1998) Purification, assembly, and localization of FtsZ. Methods Enzymol. **298**, 296–305
24 Erickson, H. P., Taylor, D. W., Taylor, K. A. and Bramhill, D. (1996) Bacterial cell division protein FtsZ assembles into protofilament sheets and minirings, structural homologs of tubulin polymers. Proc. Natl. Acad. Sci. U.S.A. **93**, 519–523
25 Mukherjee, A. and Lutkenhaus, J. (1994) Guanine nucleotide-dependent assembly of FtsZ into filaments. J. Bacteriol. **176**, 2754–2758
26 Bramhill, D. and Thompson, C. M. (1994) GTP-dependent polymerization of *Escherichia coli* FtsZ protein to form tubules. Proc. Natl. Acad. Sci. U.S.A. **91**, 5813–5817
27 Osteryoung, K. W. and McAndrew, R. S. (2001) The plastid division machine. Annu. Rev. Plant Physiol. Plant Mol. Biol. **52**, 315–333
28 Joyard, J., Billecocq, A., Bartlett, S. G., Block, M. A., Chua, N.-H. and Douce, R. (1983) Localization of polypeptides to the cytosolic side of the outer envelope membranes of spinach chloroplasts. J. Biol. Chem. **258**, 10000–10006
29 Dumas, R., Biou, V., Halgand, F., Douce, R. and Duggleby, R. G. (2001) Enzymology, structure, and dynamics of acetohydroxy acid isomeroreductase. Acc. Chem. Res. **34**, 399–408
30 Schnell, D. J. and Blobel, G. (1993) Identification of intermediates in the pathway of protein import into chloroplasts and their localization to envelope contact sites. J. Cell Biol. **120**, 103–115
31 Quardokus, E., Din, N. and Brun, Y. V. (1996) Cell cycle regulation and cell type-specific localization of the FtsZ division initiation protein in *Caulobacter*. Proc. Natl. Acad. Sci. U.S.A. **93**, 6314–6319
32 Erickson, H. P. (2001) The FtsZ protofilaments and attachment of ZipA – structural constraints on the FtsZ power stroke. Curr. Opin. Cell Biol. **13**, 55–60
33 Hale, C. A., Rhee, A. C. and de Boer, P. A. (2000) ZipA-induced bundling of FtsZ polymers mediated by an interaction between C-terminal domains. J. Bacteriol. **182**, 5153–5166
34 Bork, P., Sander, C. and Valencia, A. (1992) An ATPase domain common to prokaryotic cell cycle proteins, sugar kinases, actin, and hsp70 heat shock proteins. Proc. Natl. Acad. Sci. U.S.A. **89**, 7290–7294
35 Yu, X. C. and Margolin, W. (1997) Ca^{2+}-mediated GTP-dependent dynamic assembly of bacterial cell division protein FtsZ into asters and polymer networks *in vitro*. EMBO J. **16**, 5455–5463
36 Lu, C., Reedy, M. and Erickson, H. P. (2000) Straight and curved conformations of FtsZ are regulated by GTP hydrolysis. J. Bacteriol. **182**, 164–170
37 Addinall, S. G. and Holland, B. (2002) The tubulin ancester, FtsZ, draughtman, designer and driving force for bacterial cytokinesis. J. Mol. Biol. **318**, 219–236
38 Gueiros-Filho, F. J. and Losick, R. (2002) A widely conserved bacterial cell division protein that promotes assembly of the tubulin-like protein FtsZ. Genes Dev. **16**, 2544–2556
39 McAndrew, R. S., Froehlich, J. E., Vitha, S., Stokes, K. D. and Osteryoung, K. W. (2001) Colocalization of plastid division proteins in the chloroplast stromal compartment establishes a new functional relationship between FtsZ1 and FtsZ2 in higher plants. Plant Physiol. **127**, 1656–1666
40 Kuroiwa, H., Mori, T., Takahara, M., Miyagishima, S. Y. and Kuroiwa, T. (2002) Chloroplast division machinery as revealed by immunofluorescence and electron microscopy. Planta **215**, 185–190
41 Addinall, S. G. and Lutkenhaus, J. (1996) FtsA is localized to the septum in an FtsZ-dependent manner. J. Bacteriol. **178**, 7167–7172
42 Ma, X., Ehrhardt, D. W. and Margolin, W. (1996) Colocalization of cell division proteins FtsZ and FtsA to cytoskeletal structures in living *Escherichia coli* cells by using green fluorescent protein. Proc. Natl. Acad. Sci. U.S.A. **93**, 12998–13003
43 Vitha, S., McAndrew, R. S. and Osteryoung, K. W. (2001) FtsZ ring formation at the chloroplast division site in plants. J. Cell Biol. **153**, 111–120

Received 29 July 2004/6 December 2004; accepted 14 December 2004
Published as BJ Immediate Publication 15 December 2004, DOI 10.1042/BJ20041281